JOURNAL OF MATERIALS SCIENCE **36** (2001) 3731 – 3735

XRD, TEM, IR and ^{29}Si MAS NMR characterization of NiO-SiO_2 nanocomposites

M. CASU, A. LAI, A. MUSINU*, G. PICCALUGA, S. SOLINAS
Dipartimento di Scienze Chimiche - Universita' di CAGLIARI
E-mail: musinu@vaxca1.unica.it

S. BRUNI, F. CARIATI, E. BERETTA
Dipartimento di Chimica Inorg. Metallorg. e Analitica - Universita' di MILANO

The present study focuses on the structural properties of a NiO-SiO_2 nanocomposite with 14 mol % of nickel oxide obtained by a sol-gel method and a gradual heating the gel in the 350–900°C range. NiO nanoparticles and their dispersion in the amorphous silica matrix were studied through TEM and XRD. The behaviour at the nanoparticle/matrix interface was investigated through IR and ^{29}Si MAS NMR spectroscopy comparing the spectra of the nanocomposite with that of a silica sample obtained with the same preparation method and submitted to the same thermal treatments. The results indicate that nanoparticles, formed in cavities of the silica matrix, act as an obstacle towards the spontaneous silica polymerization process with heat treatments.

1. Introduction

Nanocomposite materials consisting of small metal or metal oxide particles dispersed in glass matrices are attracting much attention because of their potential use in a variety of fields, such as catalysis, optics, magnetism and electronics [1–4]. The properties of a nanocomposite are strongly dependent on their microstructure with regards to two main features: a) the size distribution of nanoparticles and their dispersion in the host matrix, and b) the interactions that might take place at the nanoparticle/matrix interface. For Me (or MeO)/SiO_2 materials, this kind of interaction can be related to the preparation method [4–7]. These range from the formation of "true" compounds (phyllosilicates) in systems obtained by deposition precipitation technique to the arrangement of electrostatic interactions and/or hydrogen bonds among silanol groups and water molecules close to the nanoparticles in composites obtained by sol-gel [8].

In a previous paper we reported the study of Ni-SiO_2 nanocomposites [9] in a wide range of compositions (7–80 wt % of Ni), prepared through gelation of ethanolic-tetraetoxysilane and aqueous-metal nitrate mixtures. The dried gels were submitted to a reduction treatment at 500°C in flowing hydrogen. Some difficulties were found in obtaining a homogeneous and narrow size distribution of Ni nanoparticles in composites with the highest Ni content. In order to overcome this problem, a method involving the use of nickel nitrate solutions in ethanol was undertaken. This procedure was successful in providing a good dispersion of nanosized particles also in the more concentrate system [9]. In order to explain this behaviour, the investigation of the precursors formed prior to reduction treatment is of fundamental importance, since they affect the nature of amorphous network and the possible formation of nucleation sites for nanoparticles. From this point of view, it is important to characterize the systems in their oxidized form, prior to reduction of metal ion.

We recently investigated the physical and structural properties of some metal oxide-silica (Me = Fe, Zn) nanocomposites [10–12]. In order to gain information about the presence of nanoparticle/silica interactions, we performed an IR and MAS NMR spectroscopic study [12, 13]. The spectra of the nanocomposites and silica matrices, synthesized with the same preparation method were compared. The method was successful in revealing the presence of important chemical interaction in the ZnO-SiO_2 system and of their evolution with thermal treatment [12]. On the other hand, in the Fe_2O_3-SiO_2 nanocomposites the host matrix structure resulted substantially unaltered by the presence of iron oxide nanoparticles up to $T_{treat} = 700$°C [13].

The present paper focuses on the structural properties of NiO-SiO_2 nanocomposites, with a particular attention paid to the nanoparticle/matrix interface. In order to realize a strict comparison with the structural behaviour of the metal oxide-silica (Me = Fe, Zn) nanocomposites previously investigated [10–12], the same sol gel preparation method and heat treatments were used. The amorphous and crystalline nature of the products, the occurrence of recognizable phases and the size of the particles were characterized by X-ray diffraction (XRD) and transmission electron microscopy (TEM).

*Author to whom the correspondence should be addressed.

The structural modifications of the silica matrix induced by the metal oxide were investigated through infrared (IR) and ^{29}Si MAS NMR spectroscopy.

2. Experimental

A NiO-SiO_2 composite containing 14 mol % (17 wt %) of nickel oxide was prepared by a sol gel method by mixing an ethanolic solution of tetraethoxysilane (TEOS, Aldrich 98%) with an aqueous solution of nickel nitrate ($Ni(NO_3)_2 \cdot 6H_2O$, Aldrich 98%) [9–12]. After an hour of stirring the pH of the mixture was about 4. The clear sol was poured into a teflon beaker and allowed to gel in the air. The gel was dried for about one week with the temperature slowly rising to 90°C and then powdered and kept at 150 °C for one day. The samples were heated in steps of 50°C to 500°C, and in steps of 100°C up to 900°C, keeping the temperature at each step for 30 min. The same procedure was used to prepare the silica matrix as a reference sample. NiY and SiY labels were used, where Y indicates the treatment temperature (T_{treat}). Thermogravimetric analysis carried out in air on the dried gel showed that the weight loss due the nitrate decomposition is observed at about 330 °C. Therefore only the samples heated at $T > 350$°C will be reported in the following.

The structural evolution of the samples as a function of T_{treat} was monitored by XRD using a θ–2θ conventional equipment (Siemens D500) at Mo-K_α wavelength. Nickel oxide nanoparticles were observed in the micrographs obtained using a TEM (Jeol 200CX) operating at 200 KV, after depositing the powder dispersed in octane on carbon coated grids.

Mid-IR spectra, from 4000 to 400 cm^{-1}, were obtained using a Digilab FTS-40 spectrophotometer on KBr pellets of the samples.

High resolution NMR spectra were collected using a Varian UNITY INOVA Spectrometer with a 9.39 T wide-bore Oxford magnet. The MAS experiments were performed with a probe with 7 mm ZrO_2 rotors at a spinning rate of 6 KHz. The ^{29}Si MAS experiments were run with a recycle time of 400 s, 90° pulse lengths, a 100 kHz bandwidth and 200 scans in each experiment. The ^{29}Si total integrated peak area of the spectra of SiX and NiX samples (X = 700 °C) were estimated by comparison with the ^{29}Si signal from the Si_3N_4 rotor (at about −50 ppm), with a recycle time of 500 s for each experiment.

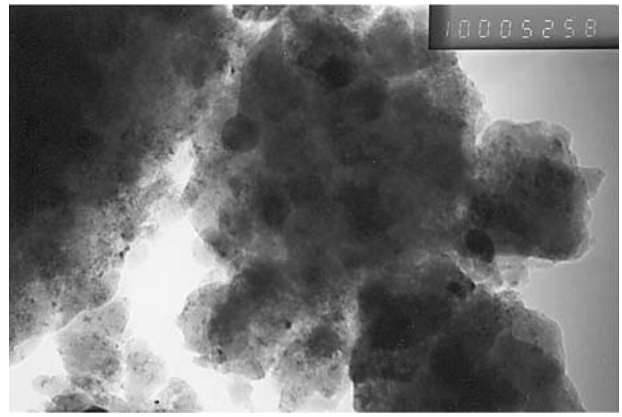

Figure 1 TEM bright field image of the Ni500 sample (×100 000).

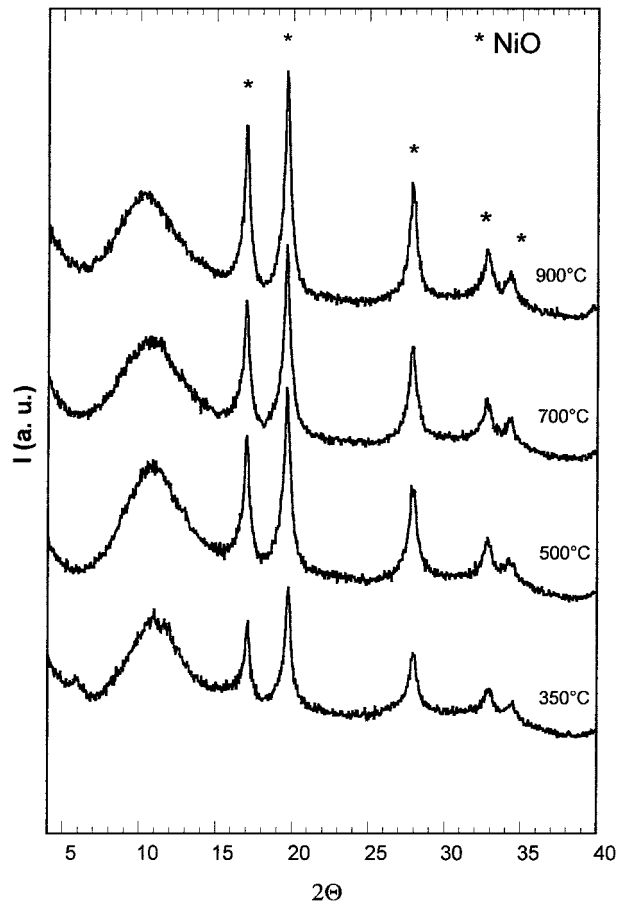

Figure 2 XRD spectra of the NiO-SiO_2 samples as a function of T_{treat}.

3. Results

TEM observations show the presence of nanoparticles dispersed over the silica matrix in all the samples. As an example, a bright field micrograph of the Ni500 sample is reported in Fig. 1, showing the nanoparticles distributed over the silica support. TEM micrographs show that the particle size increases with T_{treat}, from an average value of about 10 nm to an average of about 25–30 nm. Their distribution is large and becomes less homogeneous with the increase of T_{treat}, particularly in the Ni900 sample whose TEM images show some big (>50 nm) isolated particles.

The XRD spectra of the NiO-SiO_2 samples are reported in Fig. 2. They exhibit a series of crystalline peaks, easily ascribed to the NiO phase, superimposed to the pattern of the amorphous silica at all the T_{treat}. As the temperature increases the NiO peaks get narrower and grow with respect to the amorphous silica background which has the broad halo at about $2\theta = 11°$. In agreement with TEM observations, this is related to the increase of the nickel oxide particles. In the Ni350 spectrum a faint peak at $2\theta = 6°$ is present, which disappears at the higher temperatures. This peak is consistent with the d-spacing of $Ni(NO_3)_2 \cdot 2Ni(OH)_2$ crystalline phase [14]; also according with IR spectra reported in the following, it can be ascribed to the presence of a low amount of residual nickel nitrate which decomposes at higher heating treatment.

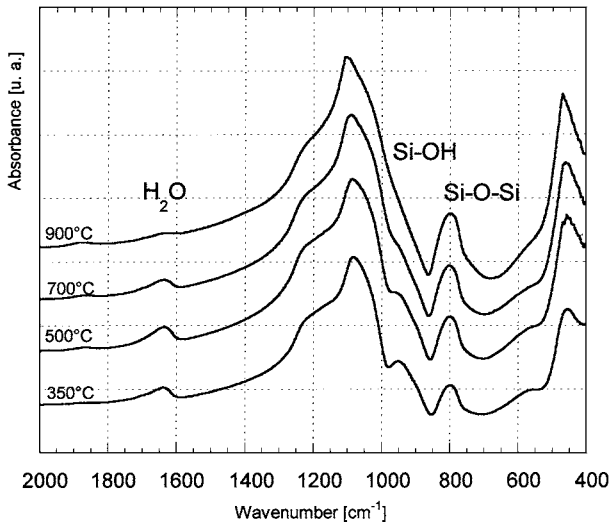

Figure 3 FT-IR spectra of KBr pellets of the NiO-SiO_2 samples as a function of T_{treat}.

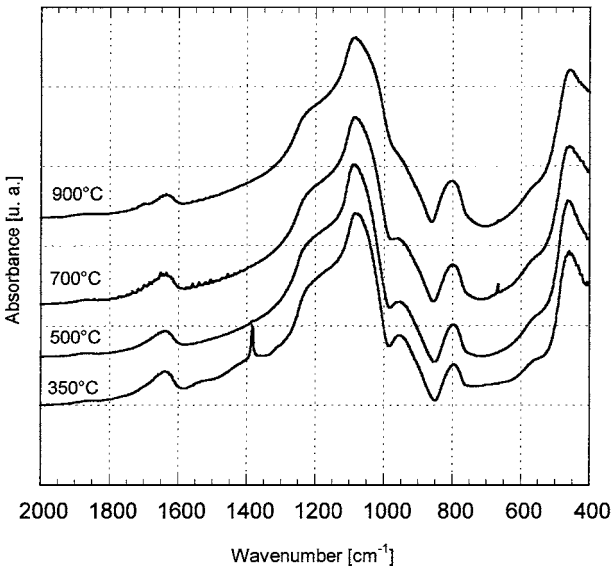

Figure 4 FT-IR spectra of KBr pellets of the SiO_2 samples as a function of T_{treat}.

The mid-IR spectra of the nanocomposites and of the corresponding silica samples, treated at the given temperatures, are reported in Figs 3 and 4 respectively. They show the bands typical of silica gel samples, with the expected modifications due to the thermal treatments [15, 16]. No major differences are apparent between the spectra of pure silica and those of the nanocomposites submitted to the same thermal treatment. The narrow band observed at 1360 cm^{-1} for Ni350 sample is due to KNO_3 [17]. This is formed by reaction between nitrate ions still present in the sample and the potassium bromide used to prepare the pellets. This spectrum exhibits also two faint bands at 1525 cm^{-1} and 1310 cm^{-1} which are absent in the spectra of samples treated at higher temperature. These signals are typical of $Ni(NO_3)_2 \cdot 2Ni(OH)_2$ crystalline [18] and are due to the presence of a residual nickel basic nitrate, in agreement with XRD data. No bands in the 600–700 cm^{-1} frequency range, like those ascribed by some authors [5, 19, 20] to the presence of nickel phyllosilicates, are present.

The band at 1640 cm^{-1}, due to the bending of the absorbed water molecules, which can interact through hydrogen bonds with silanol groups, shows a lower intensity in the samples treated at higher temperatures. Besides, it is higher in the case of nanocomposites, in agreement with the thermogravimetric analysis, which indicates an amount of absorbed water greater than that of silica samples submitted to the same thermal treatment. The intensity of the band at 950 cm^{-1}, due to the stretching of silanol groups, decreases (from 350 to 900°C) indicating the silica polycondensation process. This is also confirmed by the growing of the 795 cm^{-1} band attributed to the formation of Si-O-Si. The effects of polycondensation are however more pronounced in the spectra of silica matrix than in those of the nanocomposite.

The ^{29}Si MAS NMR spectra of the NiO-SiO_2 nanocomposite and of the corresponding silica matrix samples are shown in Fig. 5. The spectra of both series of samples show three partially overlapping signals falling in the $-80 \div -120$ ppm range, and appear more resolved in the spectra of nanocomposites. Their assignment to the Q_4, Q_3 and Q_2 groups has been made according to the literature [21]. (Qn represents the SiO_4 tetrahedron of the amorphous network which forms n bonds with neighbouring tetrahedra). The spectra of all the samples were simulated and the resulting chemical shifts and linewidths (full width at half maximum, fwhm) are reported in Table I. The chemical shift and fwhm of each spectrum of the nanocomposite and corresponding silica sample are very similar. This indicates that these ^{29}Si parameters are not affected by the presence of the paramagnetic nickel. In a previous investigation [13] it was found that the effect of paramagnetic iron (III) broaden beyond detection the signal due to the Si atoms closest to the iron oxide nanoparticles. In such event not all of the silicon atoms contribute to the observed resonances. In order to understand if nickel ion may cause this phenomenon, the same kind of experiment [13] was carried out. ^{29}Si spectra for the dried Si700 and Ni700 samples were collected, and

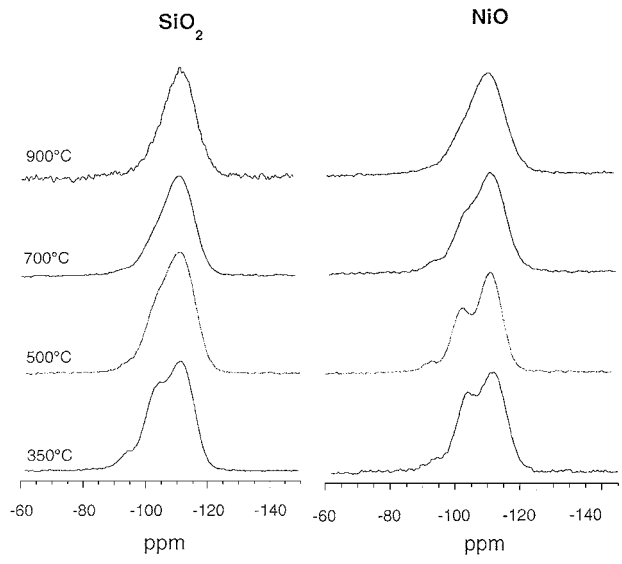

Figure 5 ^{29}Si MAS-NMR spectra of NiO-SiO_2 (right) and SiO_2 (left) samples as a function of T_{treat}.

TABLE I ^{29}Si chemical shift (δ, ppm) and full width at half maximum (fwhm, ppm) for silica matrix (Si) and nanocomposite (Ni) samples

		Q_4		Q_3		Q_2	
T_{treat}(°C)		Si	Ni	Si	Ni	Si	Ni
350	δ	−111.1	−111.0	−102.6	−102.3	−94.1	−93.0
	fwhm	8.2	8.0	6.3	6.2	5.7	5.3
500	δ	−110.6	−112.0	−102.2	−102.8	−93.7	−94.2
	fwhm	9.3	8.6	7.0	5.8	6.3	6.2
700	δ	−111.7	−113.4	−102.9	−102.7	−93.2	−92.7
	fwhm	9.1	8.7	7.6	7.7	6.8	5.8
900	δ	−112.4	−110.7	−102.0	−101.3		−92.4
	fwhm	10.0	10.1	6.5	7.2		7.0

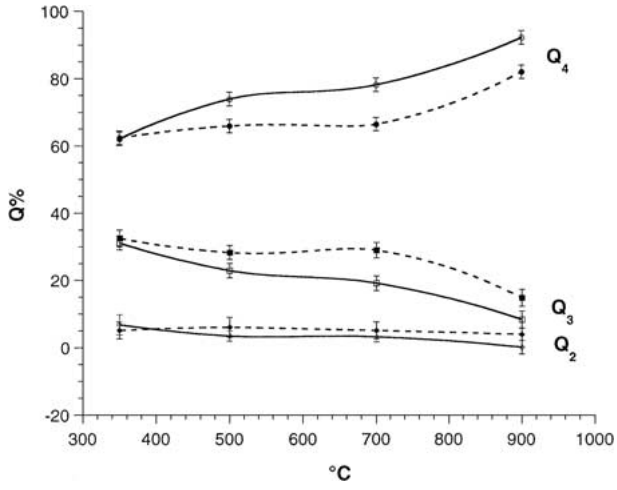

Figure 6 Relative amount of Q_n species for the SiO_2 (full symbols) and NiO-SiO_2 (open symbols) samples as a function of T_{treat}; Q_4 circles, Q_3 squares, Q_2 triangles.

the signals were compared with the ^{29}Si signal of the Si_3N_4 rotor. The integrated peak area of the Ni700 sample showed the expected reduction due to the presence of 14 mol % of NiO in the nanomomposite, in the limit of the experimental error estimated in a trial of several repeated experiments (∼3%). This result confirms that the ^{29}Si signal observed in the spectra of NiX samples corresponds to the whole amount of silicon present in the sample.

The trend of the Q*n* % as a function of T_{treat} is schematically represented in Fig. 6. As expected for silica samples obtained by sol-gel method, an increase of groups with a higher condensation degree is observed as a function of T_{treat}. Significant differences are observed for the NiO-SiO_2 samples (Fig. 6). In particular the Q_3 groups at $T_{treat} \geq 500$°C are enhanced at the expenses of Q_4 groups. Slight differences are exhibited by the Q_2 groups, which are still present in the Ni900 sample but absent in the correspondent matrix (Si900).

4. Discussion

Nanocrystalline particles with a mean size from about 10 nm up to 25–30 nm, dispersed in the amorphous silica matrix, were revealed by TEM. XRD analyses showed that the particles consist of nickel oxide phase. It is also important to outline that the particle size is similar to that previously obtained for Ni-SiO_2 nanocomposites at a given T_{treat} (500 °C) and composition [9]. The homogeneity of the dispersion is still satisfactory for the nanocomposite treated at $T_{treat} \leq 700$ °C, while in the Ni900 sample some big particles appear. This latter observation indicates that at the highest temperature the thermal stability of the nanocomposite breaks since a viscous flow of the matrix starts causing the diffusion of the oxide particles. These in some case coalesce into larger particles as big as to escape from the matrix. In any case, these unwanted effects are not so important to question the interpretation of spectroscopic data based upon the comparison of nanocomposites with the corresponding silica matrix as a function of T_{treat}.

Spectroscopic results indicate that on the whole the main features of silica are very similar in nanocomposites and silica samples. The absence of signals ascribable to Ni-O-Si contacts in the IR spectra and/or to the formation of new Q_n species in the ^{29}Si MAS NMR spectra allows to rule out the presence of a strong chemical interaction between nanoparticles and matrix. This result is in good agreement with an EXAFS investigation [22] of NiO-SiO_2 nanocomposites obtained with the same preparation method. These findings are different from others reported in the literature [5], where the formation of nickel phyllosilicates was found in nanocomposites; such samples were however sinthesized by different procedures (like deposition precipitation technique), which favour the formation of direct contacts between the dispersed phase and the host matrix.

A more quantitative analysis shows however that the distribution of the Q_n sites is significantly affected by the presence of nanoparticles as a function of temperature. In fact the percentage of the Q_4 groups is remarkably reduced in the 500–900°C range, while the Q_3 groups enhance. They grow at the expense of the Q_4 groups, which are known to increase as a function of temperature due to silica polycondensation. This is in agreement with the IR results showing that the polymerization process is hampered in nanocomposites in comparison with silica samples. Previous ^{29}Si MAS studies on silicate systems [23, 24] showed that low condensation groups are present at the matrix surface. Therefore, the present results suggest that the nanoparticles hamper the condensation of the sites that are more exposed at the interface. Moreover, IR results show the presence of a larger amount of silanol groups and water molecules in the nanocomposite with respect to the silica samples. The absorbed water can

be reasonably linked through hydrogen bonds with the silanol groups present at the matrix surface.

The overall result indicate that nickel oxide nanoparticles form in the cavities of the silica host matrix and grow with thermal treatment as a separate phase which do not directly interact with silica. Therefore, the model proposed for the nanoparticle/silica interface proposed for Fe_2O_3-SiO_2 nanocomposites holds also for the NiO-SiO_2 samples treated at low temperatures. Going to higher T_{treat}, the behaviour of the NiO-SiO_2 system is different from that observed for the previously investigated nanocomposites, mostly from ZnO-SiO_2 samples, for which a depolymerization of the matrix was caused by a reaction of zinc oxide nanoparticles at the interface [12]. As far as Fe_2O_3-SiO_2 nanocomposites is concerned, the presence of Fe-O-Si contacts was revealed by IR spectra at $T_{treat} = 900\,^{\circ}C$. This sort of interaction is absent in NiO-SiO_2 nanocomposites at all the examined T_{treat}.

5. Conclusions

The structural properties of a NiO-SiO_2 nanocomposite obtained by a sol-gel method were investigated after heating the dried gels in the 350–900 °C temperature range. The comparison of the IR and ^{29}Si MAS NMR spectra of the nanocomposite with that of a silica sample allowed to investigate the behaviour at the nanoparticle/matrix interface. The results indicate that NiO nanoparticles, formed in cavities of the amorphous silica matrix, act as an obstacle towards the spontaneous silica polymerization process and grow with thermal treatment as a separate phase which do not directly interact with silica.

Acknowledgements

This work has been supported by MURST and CNR (ROME-ITALY).

References

1. S. KOMARNENI, *J. Mater. Chem.* **2** (1992) 1219.
2. W. F. SMITH, in "Principles of Materials Science Engineering" (Mc. Graw Hill, Singapore, 1986).
3. R. W. SIEGEL, *Nanostruc. Mater.* **3** (1993) 1.
4. G. PICCALUGA, A. CORRIAS, G. ENNAS and A. MUSINU, *Material Research Foundation* **13** (2000) 1, and references therein quoted.
5. O. CLAUSE, M. KERMAREC, L. BONNEVIOT, F. VILLAIN and M. CHE, *J. Amer. Chem. Soc.* **114** (1992) 4709.
6. M. KERMAREC, J. Y. CARRIAT, P. BURATTIN, M. CHE and A. DECARREAU, *J. Phys. Chem.* **98** (1994) 12008.
7. C. R. F. LUND and J. A DUMESIC, *J. Phys. Chem.* **85** (1981) 3175.
8. C. CHANEAC, E. TRONC and J. P. JOLIVET, *J. Mater. Chem.* **6-21** (1996) 1905.
9. G. ENNAS, A. MEI, A. MUSINU, G. PICCALUGA, G. PINNA and S. SOLINAS, *J. Non-Cryst. Solids* **232** (1998) 587.
10. G. CONCAS, G. ENNAS, D. GATTESCHI, A. MUSINU, G. PICCALUGA, C. SANGREGORIO, G. SPANO, J. L. STANGER and D. ZEDDA, *Chem. Mater.* **10** (1998) 495.
11. C. CANNAS, D. GATTESCHI, A. MUSINU, G. PICCALUGA and C. SANGREGORIO, *J. Phys. Chem. B* **102-40** (1998) 7721.
12. C. CANNAS, M. CASU, A. LAI, A. MUSINU and G. PICCALUGA, *J. Mater. Chem.* **9** (1999) 1765.
13. S. BRUNI, F. CARIATI, M. CASU, A. LAI, A. MUSINU, G. PICCALUGA and S. SOLINAS, *NanoStruct. Mater.* **11-5** (1999) 573.
14. POWDER DIFFRACTION FILE, Card No. 20-0759 (Intern. Center for Diffr. Data, Swarthmore, PA).
15. A. BERTOLUZZA, C. FAGNANO, M. A. MORELLI, V. GOTTARDI and M. GUGLIELMI, *J. Non-Cryst. Solids* **48** (1982) 117.
16. D. L. WOOD and E. M. RABINOVICH, *Appl. Spectrosc.* **43** (1989) 263.
17. K. NAKAMOTO, in "Infrared Spectra of Inorganic and Coordination Compounds" (Wiley-Interscience, New York, 1970).
18. P. GALLEZOT and M. PRETTRE, *Bull Soc. Chim. Fr.* (1969) 407.
19. J. R. SOHN and A. J. OZAKI, *Catalysis* **59** (1979) 303.
20. G. WENDT, W. MOERKE, R. SCHOELLNER and H. SIEGEL, *Z. Anorg. Allg. Chem.* **43** (1980) 467.
21. E. LIPPMAA, M. MAGI, A. SAMOSON, G. ENGELHARDT and A. R. GRIMMER, *J. Amer. Chem. Soc.* **102** (1980) 4889.
22. A. CORRIAS, G. MOUNTJOY, G. PICCALUGA and S. SOLINAS, *J. Phys. Chem. B.* **103** (1999) 10081.
23. D. W. SYNDORF and G. E. MACIEL, *J. Phys. Chem.* **86** (1982) 5208.
24. J. E. MACIEL, *J. Amer. Chem. Soc.* **102** (1980) 7607.

Received 10 May 2000
and accepted 15 January 2001